CrystEngComm

Cite this: *CrystEngComm*, 2012, **14**, 4772–4776

www.rsc.org/crystengcomm

PAPER

Improving the electron mobility of TiO_2 nanorods for enhanced efficiency of a polymer–nanoparticle solar cell

Yu-Chieh Tu,[a] Jhin-Fong Lin,[a] Wei-Chun Lin,[b] Chi-Ping Liu,[b] Jing-Jong Shyue[ab] and Wei-Fang Su*[a]

Received 3rd April 2012, Accepted 18th April 2012
DOI: 10.1039/c2ce25489a

The poly(3-hexyl thiophene):TiO_2 nanorod (P3HT:TiO_2) solar cell has a better thermal stability than the P3HT:PCBM solar cell; however, the former has a lower power conversion efficiency (PCE) than the latter. We would like to enhance the PCE of P3HT:TiO_2 solar cell by improving the electron mobility of anatase TiO_2 nanorods. Two novel approaches: (1) ripening and (2) boron doping for TiO_2 nanorods were explored. TiO_2 nanorods were synthesized first by sol–gel process in the presence of an oleic acid surfactant at 98 °C for 10 h. The size of the TiO_2 nanocrystal is about 35 nm in length and 5 nm in diameter. The insulating oleic acid on the TiO_2 nanorods was replaced by pyridine (as-synthesized TiO_2) for good compatibility and charge transport between P3HT and TiO_2 in the application of hybrid P3HT:TiO_2 nanorod solar cells. The crystallinity of the as-synthesized TiO_2 nanorods was increased through ripening (120 °C, 24 h) by using an autoclave reactor while the size of the nanocrystals was not significantly changed. Boron doped TiO_2 nanorods (B-doped TiO_2) were synthesized using the same sol–gel process of as-synthesized TiO_2 nanorods but by replacing 0.7 at.% Ti with B using boron n-butoxide instead of titanium tetraisopropoxide. The UV-Vis spectroscopy and X-ray photoelectron spectroscopy (XPS) analyses indicate the B is present in TiO_2 nanorods as substitutional defects which can be either Ti–O–B or O–Ti–B bonding, with a B 1 s binding energy of 192.1 eV. The ripening process is more effective at increasing the crystallinity of TiO_2 nanorods than boron doping, as shown by XRD and Raman spectroscopy. The electron mobility of the TiO_2 nanorods is improved from 6.21×10^{-5} to 2.33×10^{-4} ($cm^2\ V^{-1}\ s$) and 5.27×10^{-4} ($cm^2\ V^{-1}\ s$) for ripened TiO_2 and B-doped TiO_2, respectively, as compared with as-synthesized TiO_2. The PCE of P3HT:TiO_2 solar cells was increased by 1.31 times and 1.79 times under A. M. 1.5 illumination for ripened and B-doped TiO_2, respectively, as compared with as-synthesized TiO_2. The B-doped TiO_2 has the highest mobility and PCE, mainly due to the presence of partially reduced Ti^{4+} by boron atom with delocalized electrons.

1 Introduction

The bulk heterojunction (BHJ) solar cell has potential to become a next-generation low cost and flexible solar cell.[1,2] Two types of BHJ solar cells have been extensively studied. One is the polymer–fullerene derivative systems, such as poly(3-hexylthiophene) (P3HT) and [6,6]-phenyl C_{61}-butyric acid methyl ester (PCBM), which have attracted most interest due to their high power conversion efficiency (PCE).[3–5] However, the morphology of polymer–fullerene derivatives is not stable upon heating which results in limited long term stability.[6] The other type is the polymer–semiconducting nanoparticle systems, such as P3HT:CdSe and P3HT:TiO_2. They usually have better thermal stability than polymer–fullerene derivative systems.[7] The P3HT:CdSe[8,9] solar cells have shown higher PCE as compared with P3HT:TiO_2 solar cells[10] due to the visible light absorption capability of CdSe nanoparticles. However, CdSe is toxic and unstable as compared with low cost and environmental friendly TiO_2. Thus, many research groups have been worked on the P3HT:TiO_2 system to improve its PCE.[11–18] One of the approaches to increase the performance of polymer–semiconducting nanoparticle solar cells is to increase the mobility of the materials. The main cause of the low cell efficiency of P3HT:TiO_2 system is due to their unbalanced carrier mobility. The mobility of TiO_2 is lower than that of P3HT by one to two orders.[7] Therefore, we would like to increase the electron mobility of TiO_2. Two approaches are explored: ripening and boron doping. Both approaches have been used for increasing the crystallinity of bulk TiO_2.[19,20] The boron doping has been studied extensively to increase the photocatalytic property of anatase TiO_2.[20–23]

[a]*No. 1, Sec. 4, Roosevelt Road, Department of Materials Science and Engineering, National Taiwan University, Taipei, 10617, Taiwan*
E-mail: suwf@ntu.edu.tw; Fax: +886 2 33664078; Tel: +886 2 33664078
[b]*No. 128, Sec. 2, Academia Road, Research Center for Applied Sciences, Academia Sinica, Taipei, 11529, Taiwan*

2 Experimental

All chemicals were purchased from Aldrich and used as received without further purification. For the thermal ripening of TiO_2 nanorods, we first synthesized TiO_2 nanorods chemically, according to the literature.[24] Here we refer to them as as-synthesized TiO_2 nanorods (as-synthesized TiO_2). Briefly, 180 g oleic acid (OA) was placed in a three-necked flask at 120 °C for 1 h to remove residual water, after which it was cooled to 98 °C. A stable mixture was obtained when 7.5 ml titanium tetra-isopropoxide (TTIP) was injected into the OA to form a pale yellow complex precursor. A 5.7 g trimethylamine-*N*-oxide dihydrate (TMAO) aqueous solution was dissolved in 25 ml deionized water. Then, TMAO solution was rapidly injected into the mixture. After stirring for 10 h, the TiO_2 nanorods were obtained. The TiO_2 nanorods were washed four times with methanol and isolated by centrifugation. Then, the nanorods were further treated with pyridine by refluxing at 70 °C for 24 h in Ar to remove oleic acid and as-synthesized TiO_2 nanorods were obtained. The as-synthesized TiO_2 nanorods were placed in an autoclave reactor (Parr Instrument Company) for ripening at 120 °C for 24 h to obtain ripened TiO_2 nanorods (ripened TiO_2). For the synthesis of boron doped TiO_2 nanorods (B-doped TiO_2), the same sol–gel process of as synthesized TiO_2 nanorods was used but by replacing 0.7 at% Ti with B using boron n-butoxide instead of the titanium tetraisopropoxide described above, and then reacted at 98 °C for 10 h under stirring. The oleic acid of synthesized nanoparticles was replaced by pyridine as described above to obtain B-doped TiO_2.

The particle size and morphology of the nanocrystals was studied by transmission electron microscopy (TEM) (FEI Tecnai G2 F20) at 200 keV. Selected-area electron diffraction (SAED) patterns were obtained to define the crystalline phase. The crystal structure of TiO_2 nanorods was determined by X-ray diffraction (XRD) (Rigaku, TTRAX III) using Cu-Kα radiation at 50 kV and 300 mA. XRD patterns were collected from 2θ between 20 and 80 with a 0.005° step at a speed of 5° min^{-1}. Raman spectra (WITec, CMR200) were obtained from TiO_2 powder by using λ = 633.6 nm for excitation. Thermogravimetric analysis (TGA) (TA Instrument, SDT-Q600) was performed from room temperature to 550 °C at a heating rate of 20 °C min^{-1} in air to determine the quantity of surface ligand of TiO_2. The spectra of X-ray photoelectron spectrometry (XPS) (ULVAC-PHI, Chigasaki) were obtained by using Al K_α radiation with a photoelectron take off angle of 45° at a high vacuum environment ($\sim 10^{-7}$ torr) to examine core-levels. The UV-Vis spectra of different TiO_2 nanorods were obtained using Perkin Elmer Lambda 35 UV/Vis spectrometer.

The devices consist of five layers with the structure of ITO/PEDOT:PSS/P3HT:TiO_2/TiO_2 nanorods/Al were fabricated accordingly to our previous study.[24] The PEDOT:PSS thin film (Baytron P, 4083) was spin coated on the cleaned ITO glass at 5000 rpm for 1 min and dried at 120 °C for 40 min. The photoactive layer was prepared by the hybrid solution of P3HT:TiO_2 nanorods with a weight ratio of 47 : 53. The P3HT was synthesized in our laboratory with molecular weight of 65 kDa, polydispersity (PDI) of 1.39 $\pm$ 0.06 and regioregularity (RR) of > 95%. The P3HT:TiO_2 nanorod films of active layer (120 nm) were spin coated on the PEDOT:PSS coated ITO. The TiO_2 nanorods layer ($\sim$ 20 nm) was subsequently cast on top of active layer as a hole blocking layer. Then, the 100 nm Al electrode was vacuum-deposited on top of the hole blocking layer to finish the fabrication of the solar cell. The electron mobility of TiO_2 is obtained by a space charge limited current (SCLC) method.[25]

3 Results and discussion

The TiO_2 nanorods were synthesized first by a sol–gel process in the presence of oleic acid surfactant at 98 °C for 10 h. The insulating oleic acid on the TiO_2 nanorods was then replaced by pyridine for good charge transport interfaces between P3HT and TiO_2 of P3HT:TiO_2 solar cell.[13] The as-synthesized TiO_2 was further heated to obtain ripened TiO_2 at 120 °C for 24 h using an autoclave. The B-doped TiO_2 was synthesized using the same sol–gel process of as-synthesized TiO_2 but by replacing 0.7 at% Ti by B in the composition of reactants (molar ratio of TTIP to boron n-butoxide is 99.3 : 0.7).

Three kinds of structures are possible for boron doping into TiO_2: (1) B substituting a Ti, (2) B substituting an O and (3) B in an interstitial position.[20–23] The substituted doping has been observed in the hydrothermal synthesis of B doped TiO_2 at 180 °C. However, the interstitial B doping occurred after the hydrothermal powder was calcined at a high temperature of 400 °C or more.[21,26] Our sol–gel synthesized B-doped TiO_2 using alkoxide precursors is expected to yield the first two kinds of substituted doping due to the low reaction temperature of 98–120 °C. The exact reaction mechanisms of B-doped TiO_2 synthesis are beyond the scope of this study. However, we would like to propose possible chemical reactions that are summarized in Scheme 1.[27] The borate ester and titanate ester are first formed after reacting their corresponding alkoxides with excess oleic acid. There are two possible routes for the two esters to react. In the first route, two esters underwent hydrolysis and condensation to form B-doped TiO_2 nanorods with a Ti–O–B linkage. The second route, the boron of borate (or the hydrolyzed form) can react with titanate (or the hydrolyzed form) to replace the water or ester of titanate to form an O–Ti–B linkage by a nucleophilic displacement reaction. Fig. 1 shows the comparison of UV-Vis spectra of different TiO_2 nanorods. The absorption edge of ripened TiO_2 moves to a shorter wavelength by 6 nm as compared with the as-synthesized TiO_2 which indicates the crystallinity of TiO_2 is increased after thermal ripening by reducing the surface defects. A red shift of 24 nm of absorption is observed for B doped TiO_2 which is the characteristic behavior of boron present in TiO_2 as substitutional to oxygen.[21,26,28]

The chemical structure of B-doped TiO_2 was further studied by XPS as shown in Fig. 2a. The B 1 s binding energy of 192.1 eV may be assigned as either Ti–O–B or O–Ti–B which is located in between TiB_2 (Ti–B: 187.5 eV) and B_2O_3 (B–O: 193.0 eV).[20,22,23,26] Fig. 2b shows the binding energy of Ti $2p^{3/2}$ peak for different type TiO_2 nanorods. The binding energy is the same for as synthesized TiO_2 nanorods and ripened TiO_2 nanorods, but it is shifted from 459.1 eV to 458.8 eV for B-doped TiO_2. The result indicates the Ti^{4+} is partially reduced with delocalized electrons by electron transfer from the boron dopant.[21]

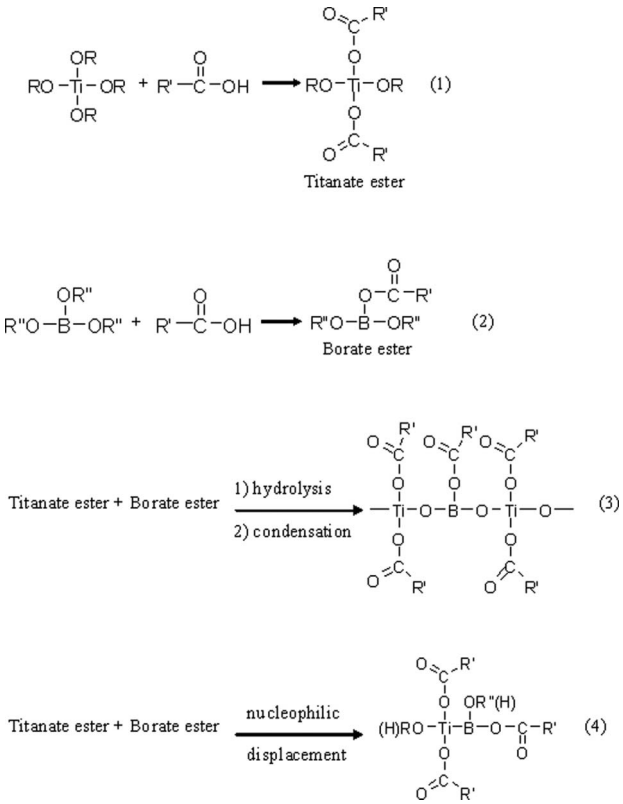

Scheme 1 Possible reactions of B doped TiO_2 sol–gel synthesis.

The amount of organics on the TiO_2 nanorods was determined by TGA as shown in Fig. 3. The results are summarized in the second column from left of Table 1. The ripened TiO_2 contains least amount of organics as compared with the other two kinds of TiO_2 which may be due to the increase of nanorod size with less surface area to accommodate surface ligands (discuss more details in below).

The size and crystalline type of different TiO_2 nanorods were studied by TEM, as shown in Fig. 4. The SAED patterns indicate they are all anatase structures. The TEM images show their size in the range of $\sim 5 \times 35$ nm. The ripening process increases the size of nanorods slightly, which means a lesser amount of surface ligands are accommodated on the surface of ripened TiO_2 nanorods. This is consistent with the TGA results. The results of

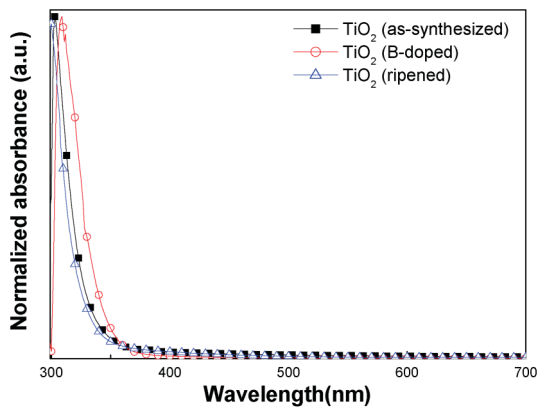

Fig. 1 UV-Vis spectra of different TiO_2 nanorods.

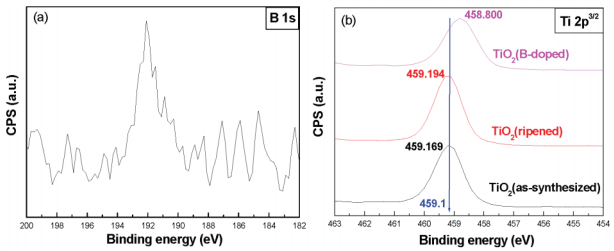

Fig. 2 XPS spectra of (a) B-doped TiO_2, and (b) Ti $2p^{3/2}$ binding for different TiO_2 nanorods.

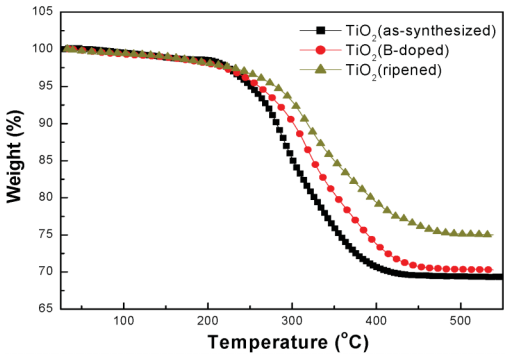

Fig. 3 TGA analysis of different TiO_2 nanorods.

TEM are summarized in the third and fourth column from the left in Table 1.

For the ripening process, the thermal energy can increase the kinetics of crystal growth of anatase TiO_2 nanorods, thus an increased crystallinity has been observed in the bulk TiO_2 through ripening.[19] The ionic radius of B^{3+} (0.02 nm) is smaller than that of Ti^{4+} (0.06 nm). The boron atoms can easily exist at the matrix of TiO_2 and reduce the amorphous regions of bulk TiO_2. Hence, the crystallinity of TiO_2 can be improved by boron doping.[20] The crystallinity of different TiO_2 nanorods in this study was investigated by XRD as shown in Fig. 5. The XRD patterns of all three TiO_2 nanorods indicate they are anatase structure. In order to compare the difference in crystallinity among the samples, we have used the same amount of TiO_2 nanorods for each measurement by weighing the sample carefully. The full width at half maximum (FWHM) of the (004) peak was calculated to show its value is, in decreasing order, ripened TiO_2 < B-doped TiO_2 < as-synthesized TiO_2, although the difference between the last two samples is not very great. The ripened TiO_2 has the best crystallinity, which is consistent with the results of the UV-Vis study. The results of the XRD study are summarized in the fifth column from the left of Table 1.

Raman spectroscopy was used to study the crystallinity of different TiO_2 nanorods further. The results are shown in Fig. 6. The spectrum of ripened TiO_2 is the best match to the spectrum of bulk single crystal anatase TiO_2[29,30] as compared with that of B-doped TiO_2 and as-synthesized TiO_2. The Raman spectra of the latter two are similar. From the results of Raman study, we can deduce that the ripened TiO_2 has the best crystallinity which is consistent with the above studies by UV-Vis and XRD.

We have examined the electron mobility of different TiO_2 nanorods using the SCLC method. The results are plotted in

Table 1 Characteristics of different TiO_2 nanorods

Sample	Wt% organics	Size by TEM (width, length)/nm	FWHM[a] of (004) peak	Mobility/$cm^2\ V^{-1}\ s^{-1}$
TiO_2 (as-synthesized)	30.60	4 ± 0.8, 33 ± 4	0.90	6.21×10^{-5}
TiO_2 (ripened)	24.70	5 ± 2.6, 39 ± 9	0.81	2.33×10^{-4}
TiO_2 (B-doped)	29.30	4 ± 1.6, 35 ± 6	0.88	5.27×10^{-4}

[a] FWHM is full width at half maximum (radian).

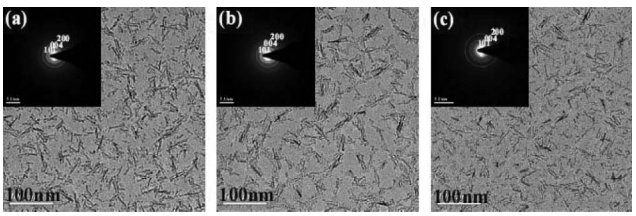

Fig. 4 TEM images of different TiO_2 nanorods (a) TiO_2 (as-synthesized), (b) TiO_2 (ripened), and (C) TiO_2 (B-doped). The insert shows the SAED patterns obtained from the image area.

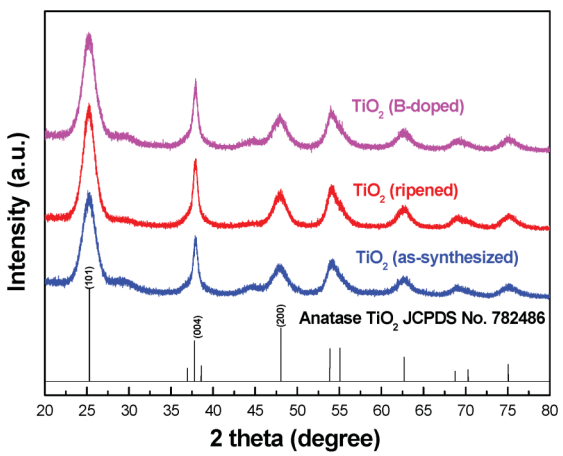

Fig. 5 XRD patterns of different TiO_2 nanorods.

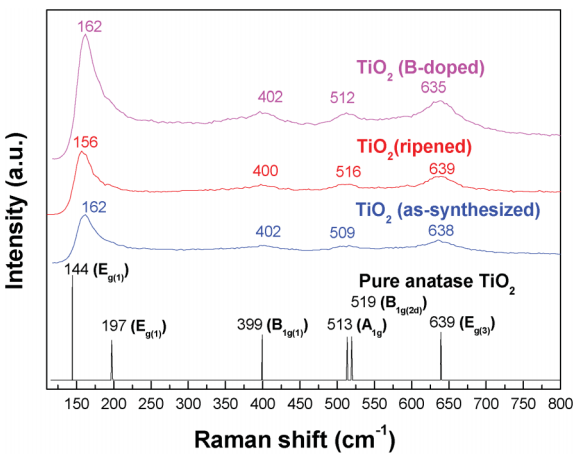

Fig. 6 Raman spectra of different TiO_2 nanorods as compared with bulk single crystal anatase TiO_2.[30]

Fig. 7 and summarized in the right column of Table 1. Both ripened TiO_2 and B-doped TiO_2 show increased electron mobility as compared to as-synthesized TiO_2, which is expected from their improved crystallinity. Furthermore, it is interesting to note that the electron mobility of B-doped TiO_2 is the highest among the three kinds of TiO_2. The result may be deduced from the presence of partially reduced Ti^{4+} by B doping and the delocalization of electrons over a few Ti atoms for ease of electron transport.[21]

These three kinds of TiO_2 nanorods were used to fabricate P3HT:TiO_2 solar cells. More than six solar cells were fabricated for each type of nanorod in order to obtain the standard deviation of the measurements. The performance of different solar cells is

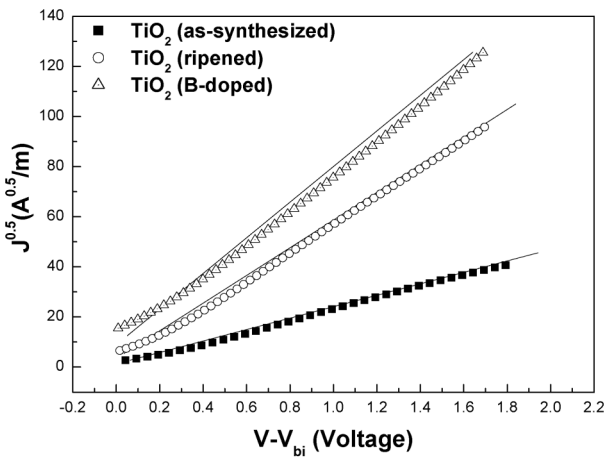

Fig. 7 Electron mobility of different TiO_2 nanorods measured by space charge limited current (SCLC) method.

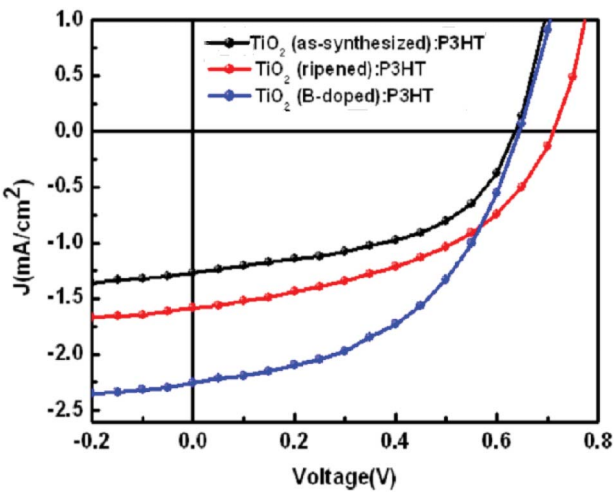

Fig. 8 *I–V* curve of different TiO_2 nanorods:P3HT solar cells.

Table 2 Performance of P3HT:TiO_2 solar cells using different TiO_2 nanorods

Sample	V_{oc}/V	J_{sc}/mA cm^{-2}	FF (%)	PCE (%)
TiO_2 (as-synthesized):P3HT	0.64 ± 0.04	1.33 ± 0.08	46.53 ± 3.40	0.39 ± 0.02
TiO_2 (ripened): P3HT	0.70 ± 0.02	1.57 ± 0.13	46.27 ± 2.35	0.51 ± 0.01
TiO_2 (B-doped): P3HT	0.63 ± 0.04	2.38 ± 0.11	46.62 ± 1.92	0.70 ± 0.02

summarized in Fig. 8 and Table 2. The PCE of solar cell has been increased by 1.31 times and 1.79 times for ripened TiO_2 and B-doped TiO_2, respectively, as compared with that of as-synthesized TiO_2. The results are expected from increased electron mobility and the improved crystalline structure of TiO_2 nanorods. The ripened TiO_2 exhibits a higher V_{oc} than the other two kinds of TiO_2 because of its low surface defects. The B-doped TiO_2 has shown the best solar cell performance as compared with as-synthesized TiO_2 and ripened TiO_2 due to its high electron mobility.

4 Conclusion

We have enhanced the performance of a P3HT:TiO_2 nanorod solar cell by improving the electron mobility of TiO_2 nanorods. Two approaches were taken: ripening, and boron doping of TiO_2 nanorods. Both approaches can increase the crystallinity of the TiO_2 nanorods, as shown by XRD. The improved crystallinity increases the mobility of TiO_2 nanorods and thus enhances their solar cell performance. The boron doping in TiO_2 nanorods can not only increase their crystallinity slightly but also provide delocalized electrons. Both results facilitate charge transport; however, the latter one is the most effective. Thus, the B-doped TiO_2 has shown the best improvement in % PCE as compared with ripened TiO_2 and as-synthesized TiO_2.

Acknowledgements

The authors thank the National Science Council of Republic of China (NSC 100-3113E-002-012) and the Yen Tjing Ling Industrial Research Institute of National Taiwan University for financial support of this research.

References

1 A. C. Mayer, S. R. Scully, B. E. Hardin, M. W. Rowell and M. D. McGehee, *Mater. Today*, 2007, **10**, 28.
2 C. J. Brabec and J. R. Durrant, *MRS Bull.*, 2008, **33**, 671.
3 M. R. Reyes, K. Kim and A. L. Carroll, *Appl. Phys. Lett.*, 2005, **87**, 083506.
4 J. H. Tsai, Y. C. Lai, T. Higashihara, C. J. Lin, M. Ueda and W. C. Chen, *Macromolecules*, 2010, **43**, 6085.
5 Y. Liang, Z. Xu, J. Xia, S. T. Tsai, Y. Wu, G. Li, C. Ray and L. Yu, *Adv. Mater.*, 2010, **22**, E135.
6 Y. C. Huang, S. Y. Chuang, M. C. Wu, H. L. Chen, C. W. Chen and W. F. Su, *J. Appl. Phys.*, 2009, **106**, 034506.
7 Y. C. Huang, W. C. Yen, Y. C. Liao, Y. C. Yu, C. C. Hsu, M. L. Ho, P. T. Chou and W. F. Su, *Appl. Phys. Lett.*, 2010, **96**, 123501.
8 W. U. Huynh, J. J. Dittmer and A. P. Alivisatos, *Science*, 2002, **295**, 2425.
9 P. Wang, A. Abrusci, H. M. P. Wong, M. Svensson, M. R. Andersson and N. C. Greenham, *Nano Lett.*, 2006, **6**, 1789.
10 Y. Y. Lin, T. H. Chu, S.-S. Li, C. H. Chuang, C. H. Chang, W. F. Su, C. P. Chang, M. W. Chu and C. W. Chen, *J. Am. Chem. Soc.*, 2009, **131**, 3644.
11 N. Kudo, S. Honda, Y. Shimazaki, H. Ohkita, H. Benten and S. Ito, *Appl. Phys. Lett.*, 2007, **90**, 183513.
12 R. Zhu, C. Y. Jiang, B. Liu and S. Ramakrishna, *Adv. Mater.*, 2009, **21**, 994.
13 Y. Y. Lin, T. H. Chu, C. W. Chen and W. F. Su, *Appl. Phys. Lett.*, 2008, **92**, 053312.
14 Y. C. Huang, J. H. Hsu, Y. C. Liao, W. C. Yen, S. S. Li, S. T. Lin, C. W. Chen and W. F. Su, *J. Mater. Chem.*, 2011, **21**, 4450.
15 M. C. Wu, H. H. Lo, H. C. Liao, S. Chen, Y. Y. Lin, W. C. Yen, T. W. Zeng, Y. F. Chen, C. W. Chen and W. F. Su, *Sol. Energy Mater. Sol. Cells*, 2009, **93**, 869.
16 T. W. Zeng, H. H. Lo, C. H. Chang, Y. Y. Lin, C. W. Chen and W. F. Su, *Sol. Energy Mater. Sol. Cells*, 2009, **93**, 952.
17 M. C. Wu, H. C. Liao, H. H. Lo, S. Chen, Y. Y. Lin, W. C. Yen, T. W. Zeng, C. W. Chen, Y. F. Chen and W. F. Su, *Sol. Energy Mater. Sol. Cells*, 2009, **93**, 961.
18 Y. C. Huang, Y. C. Liao, S. S. Li, M. C. Wu, C. W. Chen and W. F. Su, *Sol. Energy Mater. Sol. Cells*, 2009, **93**, 888.
19 G. Benko, B. Skarman, R. Wallenberg, A. Hagfeldt, V. Sundstrom and A. P. Yartsev, *J. Phys. Chem. B*, 2003, **107**, 1370.
20 J. Li, N. Lu, X. Quan, S. Chen and H. Zhao, *Ind. Eng. Chem. Res.*, 2008, **47**, 3804.
21 E. Finazzi, C. D. Valentin and G. Pacchioni, *J. Phys. Chem. C*, 2009, **113**, 220.
22 W. Zhao, W. Ma, C. Chen, J. Zhao and Z. Shuai, *J. Am. Chem. Soc.*, 2004, **126**, 4782.
23 N. Lu, X. Quan, J. Li, S. Chen, H. Yu and G. Chen, *J. Phys. Chem. C*, 2007, **111**, 11836.
24 T. W. Zeng, Y. Y. Lin, H. H. Lo, C. W. Chen, C. H. Chen, S. C. Liou, H. Y. Huang and W. F. Su, *Nanotechnology*, 2006, **17**, 5387.
25 P. N. Murgatroyd, *J. Phys. D: Appl. Phys.*, 1970, **3**, 151.
26 G. Liu, C. Sun, L. Cheng, Y. Jin, H. Lu, L. Wang, S. C. Smith, G. Q. Lu and H.-M. Cheng, *J. Phys. Chem. C*, 2009, **113**, 12317.
27 P. D. Cozzoli, A. Kornoeski and H. Weller, *J. Am. Chem. Soc.*, 2003, **125**, 14539.
28 H. Geng, S. Yin, X. Yang, Z. Shuai and B. Liu, *J. Phys.: Condens. Matter*, 2006, **18**, 87.
29 X. Chen and S. S. Mao, *Chem. Rev.*, 2007, **107**, 2891.
30 T. Ohsaka, F. Izumi and Y. Fujiki, *J. Raman Spectrosc.*, 1978, **7**, 321.

